T_1 mapping detects pharmacological retardation of diffuse cardiac fibrosis in mouse pressure-overload hypertrophy

Daniel J Stuckey, DPhil[1,2]*, Sara J McSweeney, PhD[1], May Zaw Thin, MD[1], Josef Habib, PhD[1], Anthony N Price, PhD[3], Lorna R Fiedler, PhD[1], Willy Gsell, PhD[4], Sanjay K Prasad, MD, MRCP[5] and Michael D Schneider MD, PhD[1]

[1]British Heart Foundation Centre of Research Excellence, National Heart and Lung Institute, Imperial College London, [2]Centre for Advanced Biomedical Imaging, University College London. [3]Department of Biomedical Engineering, Kings College, London, [4]Biological Imaging Centre, Medical Research Council Clinical Sciences Centre, Imperial College London, [5]Cardiovascular Magnetic Resonance Unit, Royal Brompton and Harefield NHS Foundation Trust, Imperial College London

Stuckey - MRI of cardiac fibrosis in mice

* Address for correspondence

Daniel J Stuckey

Centre for Advanced Biomedical Imaging

Paul O'Gorman Building,

University College London

72 Huntley Street

London,U.K.WC1E 6DD

Tel: 020-7679-6921 Fax 020 7679 6164

d.stuckey@ucl.ac.uk

Word count 6660

Subject codes [30 CT and MRI[124] Cardiovascular imaging agents/Techniques[130] Animal models of human disease

Abstract

Background: Diffuse interstitial fibrosis is present in diverse cardiomyopathies and associated with poor prognosis. We investigated whether MRI-based T_1 mapping could quantify the induction and pharmacological suppression of diffuse cardiac fibrosis in murine pressure-overload hypertrophy.

Methods and Results: Mice were subjected to transverse aortic constriction (TAC) or sham surgery. The angiotensin receptor blocker Losartan was given to half the animals. Cine-MRI performed at 7 and 28 days showed hypertrophy, remodeling systolic and diastolic dysfunction in TAC groups as expected. Late gadolinium-enhanced-MRI revealed focal signal enhancement at the inferior right ventricular insertion point of TAC mice concordant with the foci of fibrosis in histology. The extracellular volume fraction (ECV), calculated from pre- and post-contrast T_1 measurements, was elevated by TAC and showed direct linear correlation with picrosirius red collagen volume fraction, thus confirming the suitability of ECV as an in vivo measure of diffuse fibrosis. Treatment with Losartan reduced left ventricular dysfunction and prevented increased ECV, indicating that T_1 mapping is sensitive to pharmacological prevention of fibrosis.

Conclusions: MRI can detect diffuse and focal cardiac fibrosis in a clinically relevant animal model of pressure-overload, and is sensitive to pharmacological reduction of fibrosis by angiotensin receptor blockade. Thus, T_1 mapping can be used to assess anti-fibrotic therapeutic strategies.

Key-Words

Introduction

Persistent haemodynamic or ischemic stress leads to myocardial fibrosis [1-4]. A spectrum exists, with replacement/focal fibrosis being the predominant feature after myocardial infarction whereas in hypertrophic and dilated cardiomyopathies [1-3, 5-7], both replacement and interstitial fibrosis are present, with diffuse collagen deposition throughout the extracellular matrix [8]. Quantifying histological fibrosis from endocardial biopsies or myectomies is invasive, has inherently incomplete or non-representative sampling [1, 5], and is inapplicable to serial evaluation of small mammals. Therefore, a non-invasive technique with whole heart coverage would be highly beneficial for diagnosis, monitoring therapeutic strategies, and investigating potential counter-measures in preclinical models [6].

Late-Gadolinium enhancement MRI (LGE) can detect focal fibrosis after infarction [4, 7, 8] and distinct patterns of enhancement in cardiomyopathies [2, 9]. However for diffuse interstitial fibrosis its accuracy is reduced [1, 9-13]. Recent studies have demonstrated that pre- and post-contrast T_1 mapping can detect diffuse cardiac fibrosis in patients [5, 14-17]. As Gd-DTPA contrast agents accumulate in the increased extracellular space of fibrotic tissue [9, 11], post-contrast T_1 values are lower in areas of fibrosis [15, 16]. However, post-contrast T_1 values vary with the amount of contrast agent infused, time after injection, rate of clearance from blood, and contrast uptake into other tissues [10]. These confounding factors can be overcome by calculating the extracellular volume fraction (ECV) from T_1 measurements of the myocardium and the blood made before and after contrast administration [17, 18]. This technique has been applied to diverse forms of human heart disease [5, 14-17], was recently validated against histology in 6 transplant patients [19], and could offer a promising tool for non-invasive assessment of pharmacological therapy

Small animal CMR can provide cogent data to support clinical observations [20-27]. To validate *in vivo* T_1 mapping as a means to measure diffuse fibrosis, we performed serial cardiac MRI in

mice with pressure-overload hypertrophy induced by transverse aortic constriction (TAC). Using this model we were able to control factors that complicate or are prohibitive in studies of patients and volunteers, including the ability to image serially, before as well as after the onset of disease, and the provision of whole hearts for histological, molecular and biochemical evaluation, minimizing sample error. Our aim was to test whether *in vivo* T_1 mapping in addition to LGE-MRI could detect diffuse as well as focal cardiac fibrosis after TAC and whether both techniques were sensitive to the pharmacological reduction of fibrosis by angiotensin receptor blockade using Losartan [28, 29]. *In vivo* measurements were validated against the quantitative whole heart collagen volume fraction, myocyte cross-sectional area and quantitative RT-PCR for fibrotic and hypertrophic markers.

Methods

A detailed description of surgery, drug treatment, imaging, histology, quantitative RT-PCR and statistical analysis is provided in supplementary materials.

Surgery and drug treatment

Animal procedures complied with EU Directive 2010/63/EU and the UK Animals Scientific Procedure Act 1986 and were approved by Imperial College Animal Ethics Review Committees and the Home Office (London, UK). One week before surgery and throughout the study, half of the 12 week old male C57/BL6 mice were given Losartan (Cozaar, Merck, Frankfurt, Germany) in the drinking water (1g/L). Mice were subjected to TAC (n = 21) or sham operation (n = 8). Overall survival was 76% (sham, n = 4; TAC, n = 8; sham + Losartan, n = 4; TAC + Losartan, n = 6). Echocardiography (Vevo-770, Visualsonics, Toronto, Canada) performed two days post-surgery confirmed successful aortic constriction by the presence of a visible band around the aortic arch between the right and left common carotid arteries (CCA) (Figure 1*a & b*) and a drop in the left-to-right CCA blood flow velocity ratio (sham, 0.77 ± 0.12; TAC, 0.09 ± 0.07; p < 0.001; sham+Losartan, 0.88 ± 0.12; TAC+Losartan, 0.05 ± 0.03; p < 0.001) (Figure 1*c & d*).

Magnetic resonance imaging

Mice were imaged using a 9.4T MRI system (Agilent, Palo Alto, CA, US) and a 38 mm quadrature driven birdcage RF coil (Rapid Biomedical, Rimpar, Germany). Cardiac and respiratory gated cine-MRI was performed in the true short-axis orientation and covered the whole left ventricle (LV) as described [30]. LGE-MRI was performed 20 and 35 minutes after intraperitoneal (i.p.) injection of 0.5 mmol/kg Gd-DTPA-BMA (Omniscan. GE Healthcare, Hatfield, UK), using a multi slice inversion recovery sequence [24]. T_1 mapping was performed pre- and 25 min post-contrast injection using a fully relaxed three-slice Look-Locker inversion recovery sequence that acquired short axis gradient echo images at end-diastole at every

cardiac trigger, giving TI inversion times of ~100 ms, following a double gated non-selective adiabatic inversion pulse [24, 31] (1 mm slice thickness, TE/TR 1.6/3.2 ms; 10° excitation pulse; 40 inversion times; field of view 25.6 × 25.6 mm; matrix size 128 × 128; voxel size 200 × 200 × 1000 μm).. To allow full relaxation, at least 6s elapsed between acquisitions. Diastolic function was assessed using high temporal resolution cine-MRI [32] and Doppler echocardiography of mitral valve inflow.

Data were analysed in a blinded fashion using ImageJ (NIH, Bethesda, MD, US) and MRmap[33]. Standard measures of LV and right ventricular (RV) morphology and function were made from cine stacks. LGE-MRI images were thresholded to the full width at half maximum of enhanced regions, to identify areas of signal enhancement. For T_1 analysis, a region of interest was drawn on each image in the ventricular septum, LV free wall and blood pool of the basal, mid and apical slices pre- and post-Gd infusion. Endocardial and epicardial borders were avoided to reduce blood pool contamination, and areas of focal fibrosis identified in LGE-MRI were excluded. Unless stated otherwise, data were presented as the average of all analysed regions. Signal intensity at each inversion time was measured, points acquired during respiration removed, data fitted to the exponential curve, and T_1 calculated. Pixelwise T_1 maps were produced using the open source software MRmap[33] after in house conversion of data to DICOM. ECV was calculated from pre- and post-contrast T_1 values of myocardium and blood, correcting for the haematocrit measured at sacrifice[23].

Statistical analysis

Statistical analysis was performed with GraphPad Prism versions 5.02 and 6. Data are presented as mean ± standard deviation. Equality of variance was tested using Brown-Forsythe tests and Bartlett's tests. The majority of data showed equal variance and was analysed using two-way ANOVA with Bonferroni post-hoc test adjustment of p-values for comparisons between

the following groups: untreated vs. treated sham; untreated vs. treated TAC; untreated sham vs. treated sham; untreated TAC vs. treated TAC. Data with unequal variance were assessed using Kruskal–Wallis tests. Bivariate correlations of normally distributed data were evaluated using Pearson's test.

Results

Cardiac function

Cardiac morphology and function were measured 7 and 28 days after surgery using cine-MRI (Figure 2 & Table 1). As expected [34-36], LV end-diastolic volumes (EDV), end-systolic volumes (ESV), and masses were increased after TAC and ejection fractions were reduced. Losartan significantly attenuated the TAC-mediated increase in ESV and reduction in ejection fraction (Figure 2 & Table 1). LV stroke volumes and cardiac outputs were lower in the untreated TAC group at 7 days, although not at 28 days. Notably, LV diastolic function was impaired in untreated TAC mice at 28 days, with elevated LV peak filling rates/velocities and reduced E'/A' ratios, whereas no significant increase occurred in Losartan-treated mice (Table 1). RV function was also affected by TAC, with EDV and stroke volume reduced in untreated animals at 7 and 28 days (Table 1), changes likewise attenuated by Losartan. Hence, serial *in vivo* measurements confirmed that TAC impaired cardiac systolic and diastolic function, and that this effect was attenuated by angiotensin receptor blockade.

Late-gadolinium enhancement

In sham-operated mice, no focal regions of LGE were detected 7 or 28 days after surgery. TAC induced focal regions of LGE in 3 of 8 hearts at 7 days, increasing to 6 of 8 hearts at 28 days (p < 0.05; Figure 3). In Losartan-treated mice, TAC induced focal LGE in 3 of 6 animals by 7 days, with no further increase at 28 days, indicating that Losartan treatment did not significantly attenuate focal fibrosis. Polar map analysis (Figure 3) showed that LGE was typically located at the point where the RV inserts into the inferior LV wall (RV insertion point), as found in hypertrophic cardiomyopathy (HCM) [3, 37] and hypertensive patients [38]. The location of focal fibrosis in picrosirius red-stained tissue sections matched this specific pattern of enhancement

in the corresponding LGE images (Figure 3). To our knowledge, this is the first demonstration of verified focal fibrosis after TAC by LGE in mice.

T_1 mapping

T_1 measurements were made in the blood pool and myocardium of pre- and post-contrast inversion recovery Look-Locker acquisitions (Figure 4a-c). A pilot study into the Gadolinum kinetics was used to determine when Gd distribution was at equilibrium between the blood pool and myocardium (Figure 4d). T_1 measurements were made prior to and repeatedly after contrast administration in 6 control mice. Myocardial and blood T_1 values fell over the first 10 min, remained stable for the next 10 min, then slowly increased as contrast was cleared. Importantly, despite these changes in blood and myocardial T_1, the calculated ECV remained stable from 10 min after administration, for an hour or more (Figure 4).

The MRI acquisition protocol performed on mice at 7 and 28 days after TAC surgery is presented in Figure 4e. T_1 measurements at 7 days acquired prior to contrast administration showed a small increase in T_1 in both untreated and treated TAC hearts in all myocardial regions analysed, compared with unbanded mice, (sham, 1.26 ± 0.04s; TAC, 1.36 ± 0.05s; p < 0.05; sham+Losartan, 1.24 ± 0.06s; TAC+Losartan 1.34 ± 0.06s; p < 0.05; Fig 5 and Supp Fig 2). Pre-contrast T_1 at 7 days correlated inversely with ejection fraction (R^2 = 0.45, p < 0.001; Supp Figure 3) and was not affected by Losartan. At 28 days, no significant difference was observed..

Myocardial T_1 measured 25 min post-contrast administration was similar between groups at 7 days, was reduced 30% by TAC at 28 days, and was preserved by Losartan (sham, 0.70 ± 0.03s; TAC, 0.50 ± 0.02s; p < 0.01; sham+Losartan, 0.62 ± 0.02s; TAC+Losartan, 0.66 ± 0.03s; p = 0.39; TAC vs. TAC+Losatran, p < 0.05). T1-derived ECV was similar between groups at 7

days (Fig 5 and Supp Fig 2), was increased at 28 days in all regions of untreated TAC hearts (38% overall), and was attenuated by Losartan (sham, 16 ± 1%; TAC, 22 ± 2%, p< 0.01; sham+Losartan, 16 ± 1%; TAC+Losartan, 18 ± 4%; p = 0.38; TAC vs. TAC+Losatran, p < 0.05; Figure 5). ECV at the RV insertion points (excluded from the regional and whole heart analyses of diffuse fibrosis, in view of the focal fibrosis by LGE-MRI) also was significantly greater in untreated TAC mice but not after Losartan-treatment (sham, 16 ± 2%; TAC, 26 ± 4%; p < 0.001; sham+Losartan, 16 ± 1%; TAC+Losartan, 20 ± 4%; p = 0.33). Elevated ECV correlated with reduced ejection fractions (Supp Figure 3) and E'/A' ratios, and with increased peak LV filling velocities (Supp Figure 4), indicating the predicted impact of ECV on systolic and diastolic dysfunction. Haematocrit, essential to the calculation of ECV, showed no significant difference between groups at 28 days (Table 1). Hence, TAC acutely elevated pre-contrast T_1, possibly owing to oedema [22, 39], and chronically increased the T1-derived ECV, as anticipated for the presence of diffuse fibrosis. These latter changes were specifically reduced by angiotensin receptor blockade.

Tissue analysis

At sacrifice, heart weights and heart weight to body weight ratios were significantly greater in both TAC groups compared with controls (Table 1). Heart sections stained with picrosirius red showed the induction of extensive fibrosis throughout the myocardium by TAC (collagen volume fraction: sham, 0.4 ± 0.03%; TAC, 6.7 ± 1.5%; p < 0.001; sham+Losartan, 0.5 ± 0.02%; TAC+Losartan, 4.8 ± 2.5%; p < 0.05), which was significantly reduced by Losartan (p < 0.05 versus untreated TAC; Figure 6). Whereas collagen volume fraction calculated from tissue sections showed weak, though significant correlation with pre-contrast T_1 (R^2 = 0.24, p < 0.05), and inverse correlation with post-contrast T_1 (R^2 = 0.33, p < 0.01), there was stronger correlation between collagen volume fraction and the T1-derived ECV (R^2 = 0.57; p < 0.001; Figure 6).

A second histological parameter, myocyte cross-sectional area (CSA), was increased by TAC even with Losartan (sham, 347 ± 36 μm^2; TAC, 444 ± 48 μm^2; $p < 0.05$; sham+Losartan, 337 ± 7 μm^2; TAC+Losartan, 430 ± 62 μm^2; $p < 0.05$, Figure 7). There was a weak correlation between myocyte CSA and pre--contrast T_1 ($R^2 = 0.32$, $p < 0.01$), and post-contrast T_1 ($R^2 = 0.22$, $p < 0.05$). However, the direct linear correlation between myocyte CSA and T1-derived ECV was again stronger ($R^2 = 0.49$; $p < 0.01$; Figure 7). Likewise, there was a significant linear correlation between T1-derived ECV and molecular markers of hypertrophy (β-MHC, $R^2 = 0.36$, $p < 0.01$; ANP, $R^2 = 0.43$, $p < 0.01$).

Discussion

Accurate and sensitive detection of both replacement and interstitial fibrosis is an important clinical challenge. LGE-MRI has become the method of choice for detection of replacement fibrosis[4], while recent advances in post-contrast T_1 and ECV mapping suggest they offer a robust technique for assessment of diffuse fibrosis in patients with myocardial infarction [14, 40, 41], aortic stenosis [5, 15], adult congenital heart disease [5, 9, 14, 16, 42] and heart failure [11]. Reduced T_1 or increased ECV was also found to correlate with histological measurements of fibrosis [5, 11, 13, 19], lower ejection fraction [9, 13, 15, 42] and diastolic dysfunction [11].

Here we found that at 28, but not 7 days after induction of pressure-overload in the mouse there was a significant increase in ECV in the ventricular septum and LV free wall of basal, mid and apical LV slices. These changes were independent of focal fibrosis, as any regions of LGE were excluded from analysis [8]. Increased ECV correlated with whole heart collagen volume fraction, reduced ejection fraction, and impaired diastolic function. However, correlations within treatment groups would likely be smaller than those reported. ECV was associated with extent of hypertrophy measured by myocyte CSA and quantitative rtPCR for β-MHC and ANP. It is important to note that cardiac dysfunction and hypertrophy were relatively low in these mice [36], meaning that ECV changes are sensitive to mild forms of disease and could offer a sensitive early biomarker for a range of cardiomyopathies.

To test whether ECV was sensitive to pharmacological intervention we treated TAC mice with the angiotensin-II receptor type-1 blocker Losartan, which is known to reduce fibrosis in humans [28] and mice [29]. We found that Losartan not only attenuated histological measurements of fibrosis, but also prevented the increase in ECV, suggesting that MRI measurements of diffuse fibrosis have great potential as a non-invasive end-point for assessing novel pharmacological therapies aimed at reducing fibrosis, or for monitoring disease progression. Interestingly,

Losartan did not reduce myocyte cross-sectional area, suggesting that ECV changes are directly associated with fibrosis as opposed to hypertrophy.

Few studies have accurately detected diffuse fibrosis *in vivo* in small animal models of cardiac hypertrophy and heart failure. Using standard LGE acquisitions, diffuse fibrosis was identified in a rat model of doxorubicin cardiotoxicity [43] and an mdx mouse model of muscular dystrophy [25]. However, LGE acquisitions have limited sensitivity and are not truly quantifiable when applied to diffuse fibrosis [1, 5, 9, 11, 12, 17]. Single slice pre- and post-contrast T_1 mapping was recently applied to rats after angiotensin infusion [23] and to mice after Nω–nitro-L-arginine-methyl-ester administration or TAC [44, 45]. However, in these studies there was no exclusion of focal fibrosis, assessment of diastolic function or investigation of sensitivity to therapy. Further, in the case of chronic TAC, only four animals were studied, with no controls.

Accurate quantification of ECV requires that contrast agent is distributed equally between plasma and extracellular space. Although the usefulness of bolus followed by constant contrast infusion has been demonstrated [5], we and others [42, 46] found that a single i.p. bolus rapidly and reproducibly resulted in a dynamic equilibrium between myocardial and blood pool T_1, hence ECV calculations were accurate from 10 to at least 60 min post contrast. By removing the need for constant infusion and by using a simple *i.p.* bolus rather than *i.v.* infusion, animal sedation time was reduced and successful contrast injection within the magnet was increased. It is possible that at the Gd concentrations used in this study, transcytolemmal water exchange may result in an underestimation of ECV[45]. However, using this basic and clinically applied system we were still able to identify pharmacologically preventable elevations in ECV.

Recent studies have suggested that pre-contrast T_1 measurements can directly quantify the extent and severity of acute ischemic injury and may offer a more objective measure of area at

risk than the T_2 weighted imaging currently used [39]. Here we found that myocardial T_1 was elevated in all regions of the myocardium 7 days after TAC, hypothesized to reflect tissue oedema or more severe cellular injury with consequent release of intracellular ions into the extracellular space [22, 39] caused by pressure-induced cell death and inflammation. Increased T_1 correlated with reduced systolic function, highlighting the potential value of this measurement. Differences in T_1 lost significance by 28 days, as initial cell death and inflammation subside. It is interesting to note that pre-contrast T_1 at 7 days was elevated in the absence of increased ECV, possibly due to increased intracellular water content, rather than an extracellular increase which would likely elevate ECV. Further *in vivo* and histological validation is required but these data indicate that pre-contrast T_1 mapping could be a useful tool in quantitative assessment of tissue damage.

Although the emphasis of this report is T_1 mapping for diffuse cardiac fibrosis in mice, its use in concert with LGE for focal fibrosis is complementary. LGE has frequently been performed in small animal models of myocardial infarction [20, 24, 26], but rarely in other cardiomyopathies [25, 43] and never in mice after TAC. We found focal areas of fibrosis at the inferior RV insertion point in approximately half of the TAC mice, in agreement with findings from patients with HCM [3, 37] and hypertension [38] and is probably owing to increased mechanical wall stress at this site exacerbating damage and leading to myocyte fibre disarray, inflammation and fibrosis [38]. The ability to detect patterns of focal fibrosis with similar features to those reported for human cardiomyopathies [47] will be highly beneficial in characterisation of small animal models of HCM, DCM, myocarditis and amyloidosis, and may give greater mechanistic insight into why the focal patterns of damage occur and how they can be prevented.

The majority of studies performed on TAC mice assess cardiac function by 1D and 2D echocardiography, with few studies using cardiac MRI [34-36]. Here both were used to make

comprehensive *in vivo* measurements 7 and 28 days after TAC in untreated and Losartan treated mice. TAC induced LV chamber dilation, hypertrophy and reduced ejection fractions at 7 and 28 days. Under the conditions tested, Losartan treatment did not significantly affect EDV or LV mass, despite improvements in ESV, ejection fraction and peak ejection rate, fibrosis and ECV. This concurs with studies in other mouse models of hypertrophy, in which fibrosis was more sensitive to Losartan than LV mass [29] and highlights the importance of improved means for its assessment non-invasively. Additionally, our observation that elevated LV peak filling rates/velocities and reduced E'/A' ratios in TAC mice did not significantly differ from shams when Losartan was administered, coupled with the ECV and collagen volume fraction measurements supports the interpretation that Losartan-mediated retardation of fibrosis may improve myocardial compliance and restore diastolic relaxation, and demonstrate how advanced in vivo imaging can give insight into the processes of disease.

For more now than 20 years, the microsurgical model of pressure overload hypertrophy in mice has moved this model organism to the forefront of studies uniting pathobiological approaches with unique opportunities for genetic dissection of disease pathways and potential countermeasures. The continuous and progressive nature of pathological remodelling makes the hypertrophied heart an excellent target for pharmacological counter-measures prior to the onset of heart failure. However, methods for non-invasive, serial measurements of diffuse fibrosis have lagged behind the innovations in physiology and genetics. An accurate *in vivo* method that can monitor the effects of novel drug treatments on cardiac fibrosis would be invaluable, both for agents targeting hypertrophy and agents targeting fibrosis itself. This utility may extend to heart disease of other kinds, given the pivotal role of fibrosis in the pathogenesis of hypertrophic cardiomyopathy caused by mutations in sarcomeric protein genes [29]. Our study demonstrates that advanced small-mammal cardiac MRI offers a sensitive non-invasive tool to

detect diffuse fibrosis *in vivo,* follow its progression over time, and assess experimental therapies targeted at reducing fibrosis in the heart.

Disclosures

None

References

1.   Azevedo CF, Nigri M, Higuchi ML, Pomerantzeff PM, Spina GS, Sampaio RO, Tarasoutchi F, Grinberg M, Rochitte CE. Prognostic significance of myocardial fibrosis quantification by histopathology and magnetic resonance imaging in patients with severe aortic valve disease. *J Am Coll Cardiol*. 2011;56:278-287

2.   Assomull RG, Prasad SK, Lyne J, Smith G, Burman ED, Khan M, Sheppard MN, Poole-Wilson PA, Pennell DJ. Cardiovascular magnetic resonance, fibrosis, and prognosis in dilated cardiomyopathy. *J Am Coll Cardiol*. 2006;48:1977-1985

3.   O'Hanlon R, Grasso A, Roughton M, Moon JC, Clark S, Wage R, Webb J, Kulkarni M, Dawson D, Sulaibeekh L, Chandrasekaran B, Bucciarelli-Ducci C, Pasquale F, Cowie MR, McKenna WJ, Sheppard MN, Elliott PM, Pennell DJ, Prasad SK. Prognostic significance of myocardial fibrosis in hypertrophic cardiomyopathy. *J Am Coll Cardiol*. 2010;56:867-874

4.   Pennell DJ, Sechtem UP, Higgins CB, Manning WJ, Pohost GM, Rademakers FE, van Rossum AC, Shaw LJ, Yucel EK. Clinical indications for cardiovascular magnetic resonance (cmr): Consensus panel report. *Eur Heart J*. 2004;25:1940-1965

5.   Flett AS, Hayward MP, Ashworth MT, Hansen MS, Taylor AM, Elliott PM, McGregor C, Moon JC. Equilibrium contrast cardiovascular magnetic resonance for the measurement of diffuse myocardial fibrosis: Preliminary validation in humans. *Circulation*. 2010;122:138-144

6.   Jellis C, Martin J, Narula J, Marwick TH. Assessment of nonischemic myocardial fibrosis. *J Am Coll Cardiol*. 2010;56:89-97

7.   Wagner A, Mahrholdt H, Holly TA, Elliott MD, Regenfus M, Parker M, Klocke FJ, Bonow RO, Kim RJ, Judd RM. Contrast-enhanced mri and routine single photon emission computed tomography (spect) perfusion imaging for detection of subendocardial myocardial infarcts: An imaging study. *Lancet*. 2003;361:374-379

8.   Mewton N, Liu CY, Croisille P, Bluemke D, Lima JA. Assessment of myocardial fibrosis with cardiovascular magnetic resonance. *J Am Coll Cardiol*. 2011;57:891-903

9.   Amano Y, Takayama M, Kumita S. Contrast-enhanced myocardial t1-weighted scout (look-locker) imaging for the detection of myocardial damages in hypertrophic cardiomyopathy. *J Magn Reson Imaging*. 2009;30:778-784

10.   Gai N, Turkbey EB, Nazarian S, van der Geest RJ, Liu CY, Lima JA, Bluemke DA. T1 mapping of the gadolinium-enhanced myocardium: Adjustment for factors affecting interpatient comparison. *Magn Reson Med*. 2011;65:1407-1415

11.   Iles L, Pfluger H, Phrommintikul A, Cherayath J, Aksit P, Gupta SN, Kaye DM, Taylor AJ. Evaluation of diffuse myocardial fibrosis in heart failure with cardiac magnetic resonance contrast-enhanced t1 mapping. *J Am Coll Cardiol*. 2008;52:1574-1580

12.   Schelbert EB, Hsu LY, Anderson SA, Mohanty BD, Karim SM, Kellman P, Aletras AH, Arai AE. Late gadolinium-enhancement cardiac magnetic resonance identifies postinfarction myocardial fibrosis and the border zone at the near cellular level in ex vivo rat heart. *Circ Cardiovasc Imaging*. 2010;3:743-752

13.   Ugander M, Oki AJ, Hsu LY, Kellman P, Greiser A, Aletras AH, Sibley CT, Chen MY, Bandettini WP, Arai AE. Extracellular volume imaging by magnetic resonance imaging provides insights into overt and sub-clinical myocardial pathology. *Eur Heart J*. 2012:33:1268-1278

14.   Kellman P, Wilson JR, Xue H, Bandettini WP, Shanbhag SM, Druey KM, Ugander M, Arai AE. Extracellular volume fraction mapping in the myocardium, part 2: Initial clinical experience. *J Cardiovasc Magn Reson*. 2012;14:64

15.   Flett AS, Sado DM, Quarta G, Mirabel M, Pellerin D, Herrey AS, Hausenloy DJ, Ariti C, Yap J, Kolvekar S, Taylor AM, Moon JC. Diffuse myocardial fibrosis in severe aortic stenosis: An equilibrium contrast cardiovascular magnetic resonance study. *Eur Heart J Cardiovasc Imaging*. 2012;13:819-826

16.   Broberg CS, Chugh SS, Conklin C, Sahn DJ, Jerosch-Herold M. Quantification of diffuse myocardial fibrosis and its association with myocardial dysfunction in congenital heart disease. *Circ Cardiovasc Imaging*. 2010;3:727-734

17.   Ugander M, Oki AJ, Hsu LY, Kellman P, Greiser A, Aletras AH, Sibley CT, Chen MY, Bandettini WP, Arai AE. Extracellular volume imaging by magnetic resonance imaging provides insights into overt and sub-clinical myocardial pathology. *Eur Heart J*. 2012;33:1268-1278

18.   Arheden H, Saeed M, Higgins CB, Gao DW, Bremerich J, Wyttenbach R, Dae MW, Wendland MF. Measurement of the distribution volume of gadopentetate dimeglumine at echo-planar mr imaging to quantify myocardial infarction: Comparison with 99mtc-dtpa autoradiography in rats. *Radiology*. 1999;211:698-708

19.   Miller CA, Naish JH, Bishop P, Coutts G, Clark D, Zhao S, Ray SG, Yonan N, Williams SG, Flett AS, Moon JC, Greiser A, Parker GJ, Schmitt M. Comprehensive validation of cardiovascular magnetic resonance techniques for the assessment of myocardial extracellular volume. *Circ Cardiovasc Imaging*. 2013;6:373-383

20.   Bohl S, Lygate CA, Barnes H, Medway D, Stork LA, Schulz-Menger J, Neubauer S, Schneider JE. Advanced methods for quantification of infarct size in mice using three-dimensional high-field late gadolinium enhancement mri. *Am J Physiol Heart Circ Physiol*. 2009;296:H1200-1208

21.   Coolen BF, Geelen T, Paulis LE, Nauerth A, Nicolay K, Strijkers GJ. Three-dimensional t1 mapping of the mouse heart using variable flip angle steady-state mr imaging. *NMR Biomed*. 2010;24:154-162

22.   Messroghli DR, Nordmeyer S, Buehrer M, Kozerke S, Dietrich T, Kaschina E, Becher PM, Hucko T, Berger F, Klein C, Kuehne T. Small animal look-locker inversion recovery (salli) for simultaneous generation of cardiac t1 maps and cine and inversion recovery-prepared images at high heart rates: Initial experience. *Radiology*. 2011;261:258-265

23.   Messroghli DR, Nordmeyer S, Dietrich T, Dirsch O, Kaschina E, Savvatis K, D Oh-I, Klein C, Berger F, Kuehne T. Assessment of diffuse myocardial fibrosis in rats using small-animal look-locker inversion recovery t1 mapping. *Circ Cardiovasc Imaging*. 2011;4:636-640

24.   Price AN, Cheung KK, Lim SY, Yellon DM, Hausenloy DJ, Lythgoe MF. Rapid assessment of myocardial infarct size in rodents using multi-slice inversion recovery late gadolinium enhancement cmr at 9.4t. *J Cardiovasc Magn Reson*. 2011;13:44

25.   Stuckey DJ, Carr CA, Camelliti P, Tyler DJ, Davies KE, Clarke K. In vivo mri characterization of progressive cardiac dysfunction in the mdx mouse model of muscular dystrophy. *PLoS One*. 2012;7:e28569

26.   Stuckey DJ, Carr CA, Meader SJ, Tyler DJ, Cole MA, Clarke K. First-pass perfusion cmr two days after infarction predicts severity of functional impairment six weeks later in the rat heart. *J Cardiovasc Magn Reson*. 2011;13:38

27.   Stuckey DJ, Ishii H, Chen QZ, Boccaccini AR, Hansen U, Carr CA, Roether JA, Jawad H, Tyler DJ, Ali NN, Clarke K, Harding SE. Magnetic resonance imaging evaluation of remodeling by cardiac elastomeric tissue scaffold biomaterials in a rat model of myocardial infarction. *Tissue Eng Part A*. 2010;16:3395-3402

28. Diez J, Querejeta R, Lopez B, Gonzalez A, Larman M, Martinez Ubago JL. Losartan-dependent regression of myocardial fibrosis is associated with reduction of left ventricular chamber stiffness in hypertensive patients. *Circulation*. 2002;105:2512-2517

29. Teekakirikul P, Eminaga S, Toka O, Alcalai R, Wang L, Wakimoto H, Nayor M, Konno T, Gorham JM, Wolf CM, Kim JB, Schmitt JP, Molkentin JD, Norris RA, Tager AM, Hoffman SR, Markwald RR, Seidman CE, Seidman JG. Cardiac fibrosis in mice with hypertrophic cardiomyopathy is mediated by non-myocyte proliferation and requires tgf-beta. *J Clin Invest*. 2010;120:3520-3529

30. Stuckey DJ, Carr CA, Tyler DJ, Clarke K. Cine-mri versus two-dimensional echocardiography to measure in vivo left ventricular function in rat heart. *NMR Biomed*. 2008;21:765-772

31. Campbell-Washburn AE, Price AN, Wells JA, Thomas DL, Ordidge RJ, Lythgoe MF. Cardiac arterial spin labeling using segmented ecg-gated look-locker fair: Variability and repeatability in preclinical studies. *Magn Reson Med*. 2013;69:238-247

32. Stuckey DJ, Carr CA, Tyler DJ, Aasum E, Clarke K. Novel mri method to detect altered left ventricular ejection and filling patterns in rodent models of disease. *Magn Reson Med*. 2008;60:582-587

33. Messroghli DR, Rudolph A, Abdel-Aty H, Wassmuth R, Kuhne T, Dietz R, Schulz-Menger J. An open-source software tool for the generation of relaxation time maps in magnetic resonance imaging. *BMC Med Imaging*. 2010;10:16

34. Aksentijevic D, Lygate CA, Makinen K, Zervou S, Sebag-Montefiore L, Medway D, Barnes H, Schneider JE, Neubauer S. High-energy phosphotransfer in the failing mouse heart: Role of adenylate kinase and glycolytic enzymes. *Eur J Heart Fail*. 2010;12:1282-1289

35. Diwan A, Wansapura J, Syed FM, Matkovich SJ, Lorenz JN, Dorn GW, 2nd. Nix-mediated apoptosis links myocardial fibrosis, cardiac remodeling, and hypertrophy decompensation. *Circulation*. 2008;117:396-404

36. van Nierop BJ, van Assen HC, van Deel ED, Niesen LB, Duncker DJ, Strijkers GJ, Nicolay K. Phenotyping of left and right ventricular function in mouse models of compensated hypertrophy and heart failure with cardiac mri. *PLoS One*. 2013;8:e55424

37. Choudhury L, Mahrholdt H, Wagner A, Choi KM, Elliott MD, Klocke FJ, Bonow RO, Judd RM, Kim RJ. Myocardial scarring in asymptomatic or mildly symptomatic patients with hypertrophic cardiomyopathy. *J Am Coll Cardiol*. 2002;40:2156-2164

38. Blyth KG, Groenning BA, Martin TN, Foster JE, Mark PB, Dargie HJ, Peacock AJ. Contrast enhanced-cardiovascular magnetic resonance imaging in patients with pulmonary hypertension. *Eur Heart J*. 2005;26:1993-1999

39. Dall'Armellina E, Piechnik SK, Ferreira VM, Si QL, Robson MD, Francis JM, Cuculi F, Kharbanda RK, Banning AP, Choudhury RP, Karamitsos TD, Neubauer S. Cardiovascular magnetic resonance by non contrast t1-mapping allows assessment of severity of injury in acute myocardial infarction. *J Cardiovasc Magn Reson*. 2012;14:15

40. Messroghli DR, Niendorf T, Schulz-Menger J, Dietz R, Friedrich MG. T1 mapping in patients with acute myocardial infarction. *J Cardiovasc Magn Reson*. 2003;5:353-359

41. Messroghli DR, Walters K, Plein S, Sparrow P, Friedrich MG, Ridgway JP, Sivananthan MU. Myocardial t1 mapping: Application to patients with acute and chronic myocardial infarction. *Magn Reson Med*. 2007;58:34-40

42. Jerosch-Herold M, Sheridan DC, Kushner JD, Nauman D, Burgess D, Dutton D, Alharethi R, Li D, Hershberger RE. Cardiac magnetic resonance imaging of myocardial contrast uptake and blood flow in patients affected with idiopathic or familial dilated cardiomyopathy. *Am J Physiol Heart Circ Physiol*. 2008;295:H1234-H1242

43. Lightfoot JC, D'Agostino RB, Jr., Hamilton CA, Jordan J, Torti FM, Kock ND, Workman S, Hundley WG. Novel approach to early detection of doxorubicin cardiotoxicity by

gadolinium-enhanced cardiovascular magnetic resonance imaging in an experimental model. *Circ Cardiovasc Imaging*. 2010;3:550-558

44.   Coelho-Filho OR, Shah RV, Mitchell R, Neilan TG, Moreno H, Jr., Simonson B, Kwong RY, Rosenzweig A, Das S, Jerosch-Herold M. Quantification of cardiomyocyte hypertrophy by cardiac magnetic resonance: Implications on early cardiac remodeling. *Circulation*. 2013;128:1225-1233

45.   Coelho-Filho OR, Mongeon FP, Mitchell R, Moreno H, Jr., Nadruz W, Jr., Kwong R, Jerosch-Herold M. Role of transcytolemmal water-exchange in magnetic resonance measurements of diffuse myocardial fibrosis in hypertensive heart disease. *Circ Cardiovasc Imaging*. 2013;6:134-141

46.   Schelbert EB, Testa SM, Meier CG, Ceyrolles WJ, Levenson JE, Blair AJ, Kellman P, Jones BL, Ludwig DR, Schwartzman D, Shroff SG, Wong TC. Myocardial extravascular extracellular volume fraction measurement by gadolinium cardiovascular magnetic resonance in humans: Slow infusion versus bolus. *J Cardiovasc Magn Reson*. 2011;13:16

47.   Vohringer M, Mahrholdt H, Yilmaz A, Sechtem U. Significance of late gadolinium enhancement in cardiovascular magnetic resonance imaging (cmr). *Herz*. 2007;32:129-137

Table 1

Table 1: Cardiac morphology and function measured at 7 & 28 days post-surgery. Mean ± s.d.

*p < 0.05, **p < 0.01, ***p < 0.005 sham vs. TAC, #p < 0.05 untreated vs. Losartan.

	day	Sham (n = 4)	TAC (n = 8)	Sham+Losartan (n = 4)	TAC+Losartan (n = 6)
LV function					
EDV (µl)	7	61 ± 10	67 ± 6	48 ± 5	63 ± 7
	28	60 ± 6	**79 ± 2****	53 ± 4	**72 ± 4****
ESV (µl)	7	15 ± 2	**37 ± 8*****	10 ± 3	**25 ± 6**,#**
	28	14 ± 3	**43 ± 3*****	12 ± 2	**32 ± 4**,#**
SV (µl)	7	45 ± 8	**30 ± 5****	38 ± 5	38 ± 6
	28	46 ± 4	36 ± 3	41 ± 3	42 ± 2
EF (%)	7	75 ± 1	**45 ± 3****	78 ± 3	**59 ± 3**,#**
	28	78 ± 2	**46 ± 4*****	78 ± 2	**58 ± 3**,#**
Heart Rate (bpm)	7	528 ± 35	545 ± 30	519 ± 31	503 ± 41
	28	556 ± 23	564 ± 12	568 ± 13	534 ± 13
Cardiac output (ml/min)	7	23 ± 2	**16 ± 3****	18 ± 3	19 ± 3
	28	26 ± 1	20 ± 2	24 ± 2	23 ± 1
LV filling/ejection					
peak ejection rate (ul/s)	28	375 ± 19	**263 ± 40***	372 ± 63	304 ± 72
peak filling rate (ul/s)	28	347 ± 42	**450 ± 50***	311 ± 64	**470 ± 59***
E/A ratio	28	1.14 ± 0.23	**0.70 ± 0.23***	1.13 ± 0.22	0.79 ± 0.21
Peak filling velocity(mm/s)	28	664 ± 136	**1176 ± 226***	899 ± 106	1069 ± 276

RV Function

EDV (µl)	7	51 ± 7	**39 ± 4***	47 ± 9	43 ± 6
	28	55 ± 8	**46 ± 5***	55 ± 8	49 ± 8
ESV (µl)	7	9 ± 1	9 ± 2	10 ± 2	7 ± 3
	28	9 ± 2	13 ± 7	12 ± 1	8 ± 4
SV (µl)	7	42 ± 7	**30 ± 5***	36 ± 8	36 ± 5
	28	46 ± 6	**33 ± 5***	43 ± 7	41 ± 7
EF (%)	7	82 ± 2	77 ± 7	78 ± 5	84 ± 6
	28	83 ± 3	73 ± 11	77 ± 2	84 ± 8

Weights

LV mass (mg)	7	118 ± 7	**148 ± 11****	108 ±16	**145 ± 14****
	28	114 ± 8	**145 ± 26***	101 ± 11	**155 ± 20****
LV mass/EDV (mg/ µl)	7	2.0 ± 0.4	2.2 ± 0.2	2.3 ±0.3	2.3 ± 0.5
	28	2.0 ± 0.4	1.8 ± 0.2	1.9 ± 0.1	2.1 ± 0.3
Body weight (g)	7	22 ± 1	23 ± 1	23 ± 1	21 ± 1
	28	27 ± 1	26 ± 1	25 ± 1	25 ± 1
LV mass:body wt ratio	7	4.3 ± 1	**5.6 ± 1***	4.3 ± 1	**5.8 ± 1***
	28	4.2 ± 1	**5.7 ± 1***	4.1 ± 1	**6.1 ± 1***
heart weight (mg)	28	190 ± 3	**247 ± 3***	161 ± 3	**218 ± 2***
heart wt:body wt ratio	28	7.1 ± 1	**9.4 ± 1***	6.5 ± 1	**8.7 ± 1***
haematocrit (%)	28	44 ± 2	44 ± 3	43 ± 2	44 ± 1

Figure 1: Transthoracic ultrasound of the aortic arch of sham (*a*) and TAC (*b*) mice 2 days after surgery. Arrow indicates the band. *c:* 2D guided Doppler was used to measure blood flow in right and left common carotid artery (CCA). Time scale in seconds. *d:* The ratio of left CCA to right CCA was reduced in all banded mice. Scale bar 1 mm. ***p < 0.005 sham vs. TAC.

Figure 2: *a:* End diastolic and end systolic cine-MR images from untreated and Losartan treated sham and TAC mice 28 days after surgery. Scale bar 1mm. *b:* Cine-MRI measurements of cardiac morphology and function made at 7 and 28 days post TAC. *p < 0.05, **p < 0.01, ***p < 0.005 sham vs. TAC, #p < 0.05 untreated vs. Losartan. Sham n=4, TAC n=8, sham+Losartan n=4, TAC+Losartan n=6.

Figure 3: LGE-MRI (*a*) and picrosirius red staining (*b*) identified focal fibrosis in TAC mice predominately at the RV insertion point. Scale bar, 1mm. *c*. Polar plots of the distribution and extent of LGE in all TAC mice at 7 and 28 days.

Figure 4: *a:* Selection of images acquired at increasing inversion times after a global inversion pulse made using a Look-locker inversion recovery acquisition before and 25 mins after i.p. Gd injection. Far right panel shown T_1 maps calculated from the images. *b & c:* Signal intensity curves from myocardium and blood pool pre and post contrast were used to calculate T1. *d:* Serial myocardial and blood pool T_1 measurements after i.p. Gd injection were used to calculate ECV (n = 6). *e:* MRI acquisition protocol for TAC study.

Figure 5: *a:* Pre and post contrast T_1 maps from sham and TAC mice. Colour scale bar shows T1 from 0 to 2000 ms. *b:* T_1 pre-contrast, *c:* T_1 post contrast, and *c;* ECV measurements (average of all regions) made 7 and 28 days after surgery in sham ,TAC and Losartan treated mice. *p < 0.05, **p < 0.01 sham vs. TAC, #p < 0.05 Untreated vs. Losartan. Sham n=4, TAC n=8, sham+Losartan n=4, TAC+Losartan n=6.

Figure 6: *a:* Representative picrosirius red stained heart sections from all groups (left and middle) and thresholded image from TAC showing collagen (right). Scale bar, 1mm *b:* Collagen volume fraction increased after TAC and reduced by Losartan treatment. *p < 0.05, ***p < 0.005 compared to sham, #p < 0.05 compared to untreated TAC. *c: In vitro* measurement of collagen volume fraction correlated with *in vivo* measurement of ECV. Sham n=4, TAC n=8, sham+Losartan n=4, TAC+Losartan n=6.

Figure 7: *a:* Dystrophin stain hearts sections used for measurement of myocyte cross sectional area. *b*: CSA was elevated at 28 days post-surgery in TAC mice. $*p < 0.05$. *c:* CSA directly correlated with ECV. Sham n=4, TAC n=8, sham+Losartan n=4, TAC+Losartan n=6..
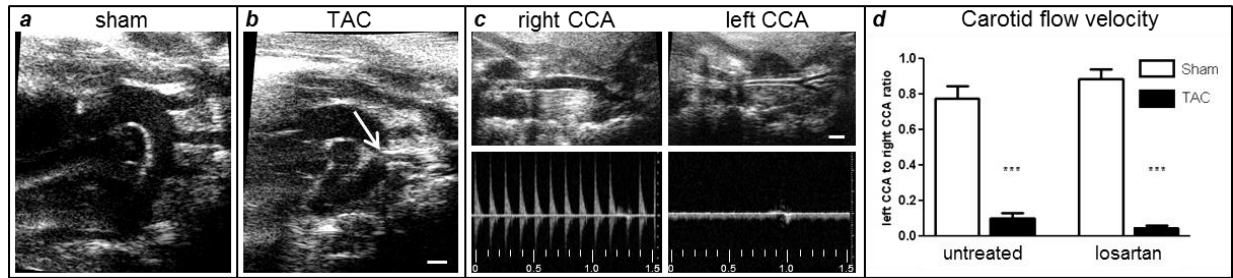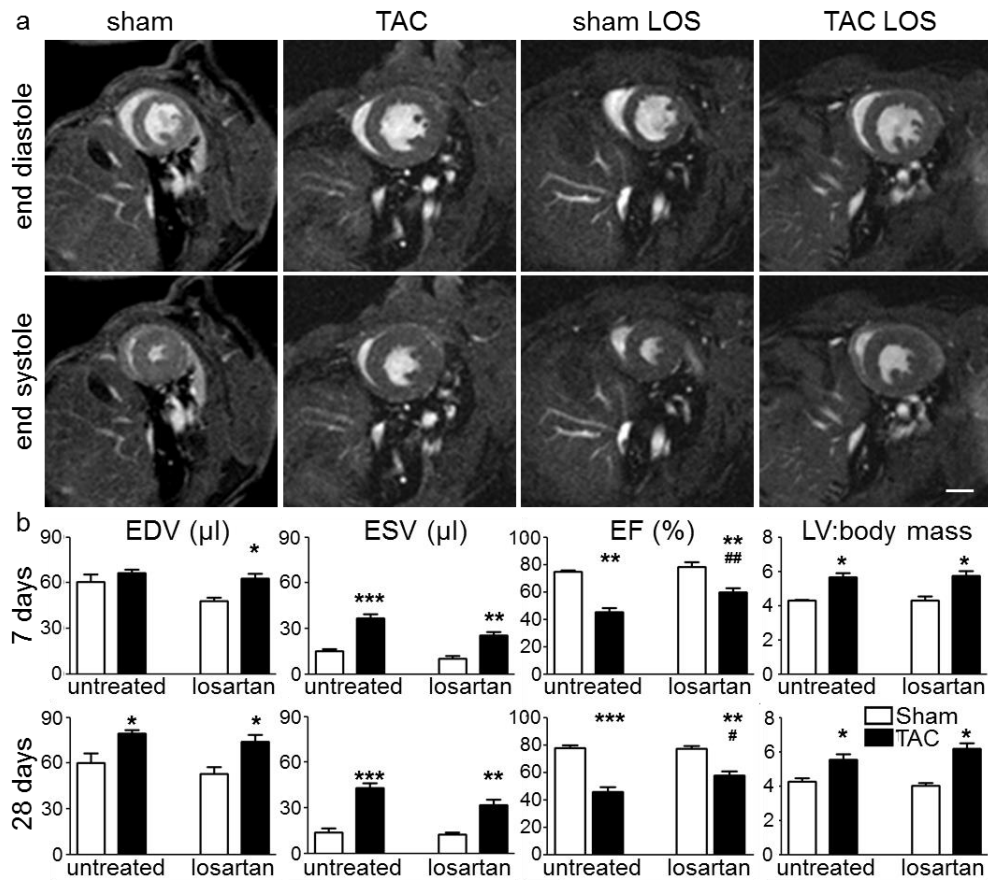
Figure 1

Figure 1: Transthoracic ultrasound of the aortic arch of sham (*a*) and TAC (*b*) mice 2 days after surgery. Arrow indicates the band. *c:* 2D guided Doppler was used to measure blood flow in right and left common carotid artery (CCA). Time scale in seconds. *d:* The ratio of left CCA to right CCA was reduced in all banded mice. Scale bar 1 mm. ***$p < 0.005$ sham vs. TAC.

Figure 2

Figure 2: *a:* End diastolic and end systolic cine-MR images from untreated and Losartan treated sham and TAC mice 28 days after surgery. Scale bar 1mm. *b:* Cine-MRI measurements of cardiac morphology and function made at 7 and 28 days post TAC. *p < 0.05, **p < 0.01, ***p < 0.005 sham vs. TAC, #p < 0.05 untreated vs. Losartan. Sham n=4, TAC n=8, sham+Losartan n=4, TAC+Losartan n=6.
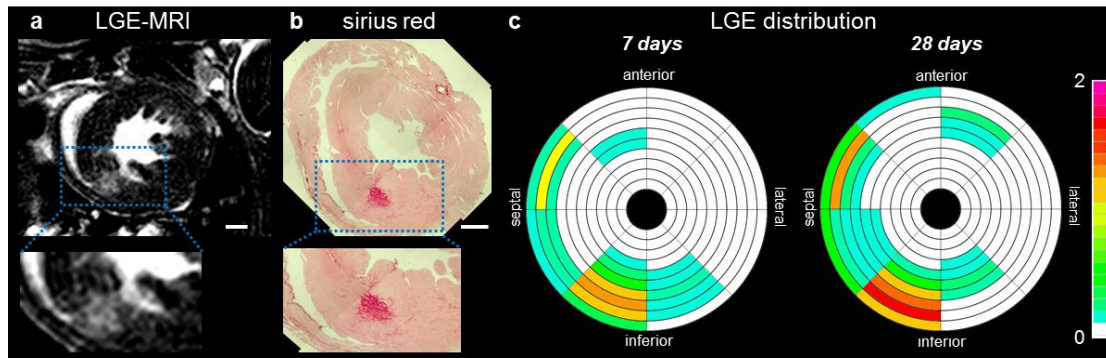
Figure 3

Figure 3: LGE-MRI (*a*) and picrosirius red staining (*b*) identified focal fibrosis in TAC mice predominately at the RV insertion point. Scale bar, 1mm. *c*. Polar plots of the distribution and extent of LGE in all TAC mice at 7 and 28 days.
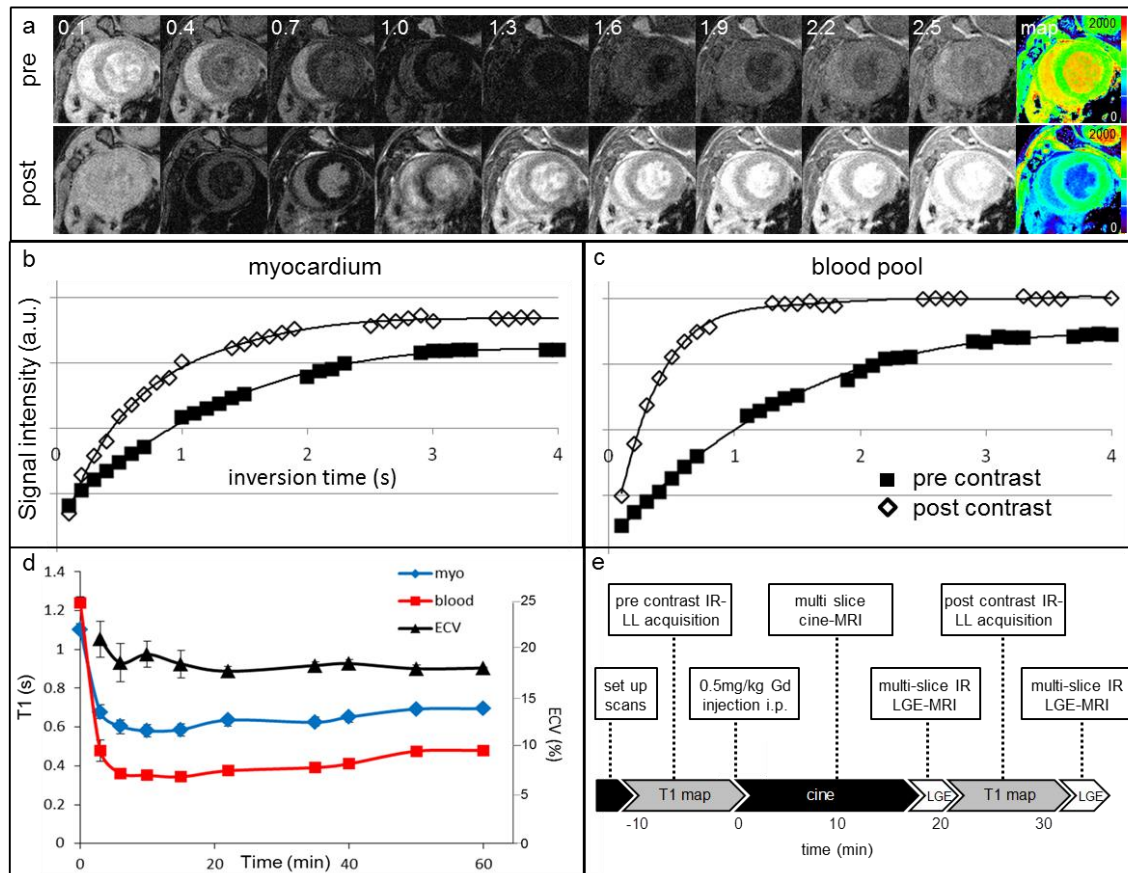
.

Figure 4

Figure 4: *a:* Selection of images acquired at increasing inversion times after a global inversion pulse made using a Look-locker inversion recovery acquisition before and 25 mins after i.p. Gd injection. Far right panel shown T$_1$ maps calculated from the images. *b & c:* Signal intensity curves from myocardium and blood pool pre and post contrast were used to calculate T1. *d:* Serial myocardial and blood pool T$_1$ measurements after i.p. Gd injection were used to calculate ECV (n = 6). *e:* MRI acquisition protocol for TAC study.
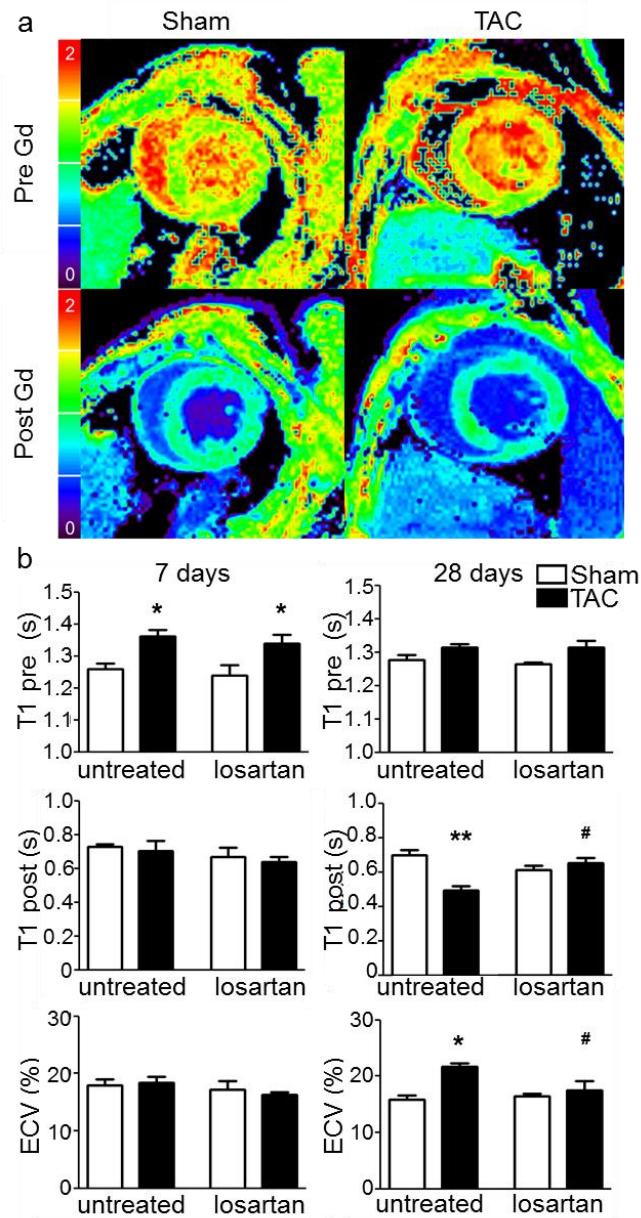
Figure 5

Figure 5: **a:** Pre and post contrast T_1 maps from sham and TAC mice. Colour scale bar shows T1 from 0 to 2000 ms. **b:** T_1 pre-contrast, **c:** T_1 post contrast, and **c;** ECV measurements (average of all regions) made 7 and 28 days after surgery in sham ,TAC and Losartan treated mice. *p < 0.05, **p < 0.01 sham vs. TAC, #p < 0.05 Untreated vs. Losartan. Sham n=4, TAC n=8, sham+Losartan n=4, TAC+Losartan n=6.
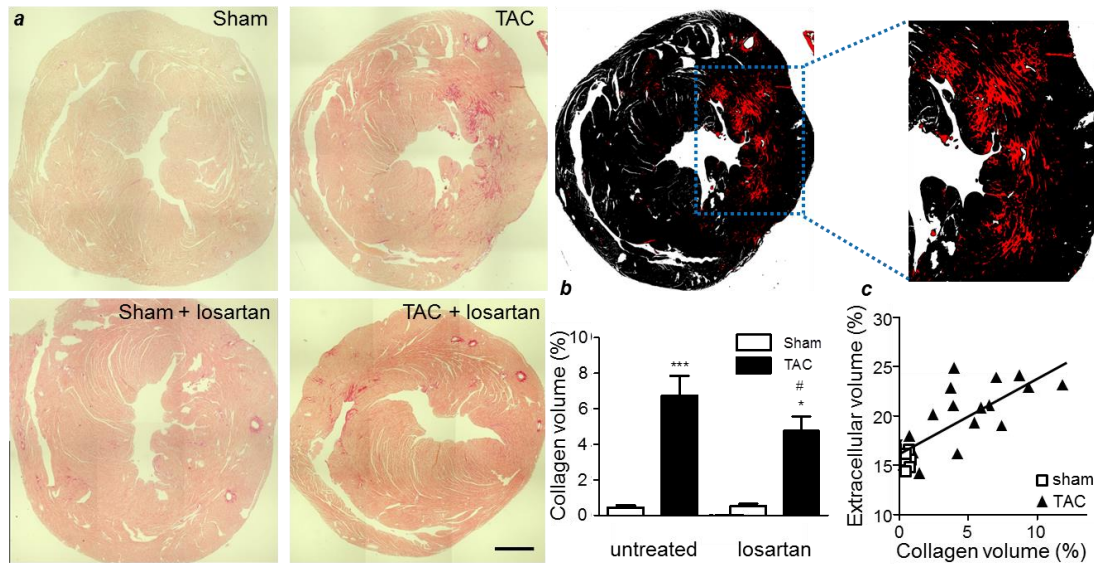
Figure 6

Figure 6: ***a:*** Representative picrosirius red stained heart sections from all groups (left and middle) and thresholded image from TAC showing collagen (right). Scale bar, 1mm ***b:*** Collagen volume fraction increased after TAC and reduced by Losartan treatment. *p < 0.05, ***p < 0.005 compared to sham, #p < 0.05 compared to untreated TAC. ***c:*** *In vitro* measurement of collagen volume fraction correlated with *in vivo* measurement of ECV. Sham n=4, TAC n=8, sham+Losartan n=4, TAC+Losartan n=6.
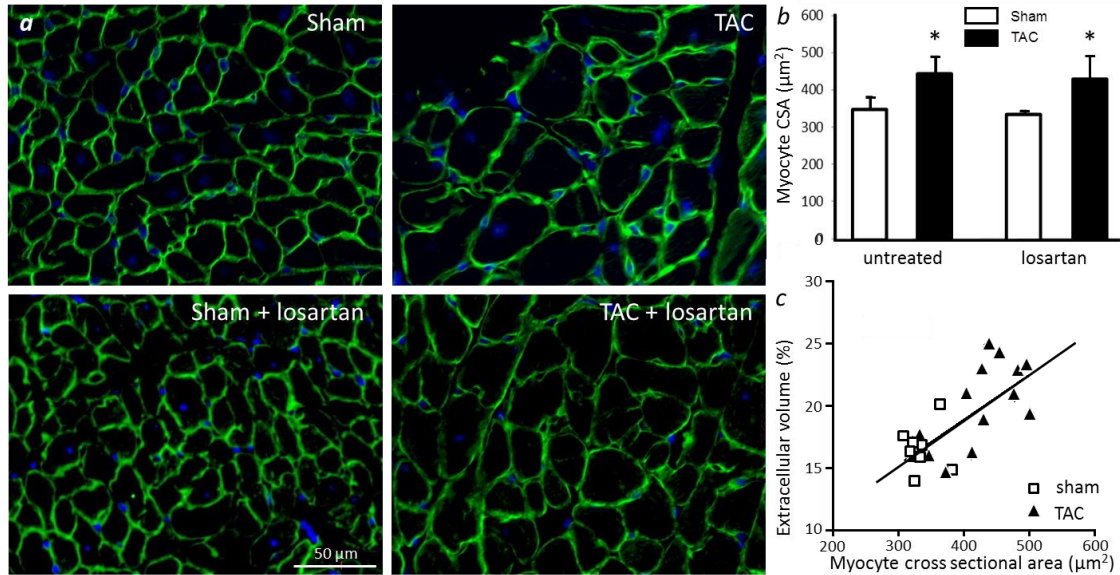
Figure 7

Figure 7: *a:* Dystrophin stain hearts sections used for measurement of myocyte cross sectional area. *b*: CSA was elevated at 28 days post-surgery in TAC mice. *p < 0.05. *c:* CSA directly correlated with ECV. Sham n=4, TAC n=8, sham+Losartan n=4, TAC+Losartan n=6..